

# Factors affecting crystallization of bioactive glasses

Hanna Arstila, Erik Vedel, Leena Hupa\*, Mikko Hupa

*Process Chemistry Centre, Åbo Akademi University, Biskopsgatan 8, FI-20500, Turku, Finland*

Available online 5 June 2006

## Abstract

The product range of bioactive glasses is restricted by their tendency to crystallize at working processes typically performed with high viscosity melts. In this work high-temperature properties viscosity, devitrification temperature and liquidus temperature of seven bioactive glasses are measured. Further, the parameters used to describe glass stability and crystallization tendency are discussed. The results indicate that bioactive glasses can be divided into two groups: (1) glasses which nucleate and crystallize within the whole viscosity range of interest for forming processes, such as sintering and fiber drawing, and (2) glasses with a viscosity range enabling high temperature processing without crystallization. The main difference between these groups is the primary crystalline phase in crystallization. Glasses showing sodium-calcium-silicate crystallization are sensitive to high temperature processing, while glasses showing wollastonite crystallization have better stability at working temperatures. Thus, by adjusting the composition special products, such as fibers and porous implants can be manufactured.

© 2006 Elsevier Ltd. All rights reserved.

**Keywords:** Sintering; Fibres; Glass; Biomedical applications

## 1. Introduction

Since the breakthrough of bioactive glasses as bone implant materials in the 1970s, there has also been a growing interest to apply these special glasses in other applications.<sup>1</sup> The first bioactive glasses made of sodium oxide, calcium oxide, phosphorous pentoxide and silicon dioxide were found to phase separate and crystallize easily during working processes in the temperature range between glass transformation and liquidus.<sup>2</sup> The energy provided from heating during working processes assists in breaking bondings in the glass network structure and thus facilitates arranging the melt into crystal structures in this unstable region. Compared to traditional glasses bioactive glasses have a high amount of network modifiers and a low amount of silica network formers, thus giving smaller structural units. Phosphorous pentoxide affects the crystallization of silicate glasses in two ways. Basically it is a glass network former, but the double oxygen bond is assumed to favor phosphate phase formation and thus increase the tendency towards crystallization.<sup>3</sup> High temperature working range of bioactive glasses has been increased by additions of potassium oxide, magnesium oxide or boron oxide.<sup>4</sup> This wider composition range enabled the manufacture

of porous implants made by sintering of glass microspheres.<sup>5</sup> The bioactivity of these sintered bodies has been tested *in vivo*.<sup>6</sup> The increased workability often means also changes in the bioactivity of the glass leading to only medium or low bioactivity.<sup>7</sup> Although the understanding of the influence of different components on both the bioactivity and the working properties has increased, still the most clinically used bioactive glasses are plates, granules and powdered glass, i.e. products which do not require any special heat treatment during manufacture.

Sintering of porous bodies from crushed glass or drawing of fibers from preforms or glass melts requires closely controlled isothermal conditions at typical viscosity levels. In sintering the glass particles are passed directly from room temperature to the pre-heated furnace at a temperature depending on the glass composition.<sup>8</sup> Temperatures usually applied for sintering of porous bodies through viscous flow corresponds to roughly  $10^8$  dPas.<sup>9</sup> However, several typical bioactive glasses devitrify already at higher viscosities.<sup>10</sup>

Fiber drawing is usually performed at viscosity values between  $10^2$  and  $10^4$  dPas.<sup>9,11</sup> Downdrawing of fibers from melt or solid preform is usually accomplished with strong melts showing moderate change of viscosity with temperature.<sup>12</sup> However, bioactive glasses of low silica content form fragile melts, thus showing a marked increase of viscosity with decreasing temperature. Fiber manufacture from fragile melts requires updrawing from a supercooled melt or a rapid quenching of fibers.<sup>12</sup>

\* Corresponding author. Tel.: +358 215 4563; fax: +358 215 4962.  
E-mail address: [leena.hupa@abo.fi](mailto:leena.hupa@abo.fi) (L. Hupa).

Parameters typical for crystal nucleation and growth are important for characterization of high-temperature properties. Stability of glasses against crystallization upon reheating is often described with relative values calculated from the temperatures of glass transformation, liquidus and crystallization.<sup>13,14</sup> The shape and dimensionality of crystal growth are estimated from activation energy and Avrami constant.<sup>15–17</sup>

In this work different crystal forming characteristics measured with thermal analysis are compared with observations from heat-treated samples. The influence of glass composition on the primary phases formed at crystallization is discussed. The goal is to gain information needed to choose bioactive glasses suitable for fiber drawing and sintering processes.

## 2. Experimental

The experiments were performed with two reference and five novel glasses (Table 1). The batches mixed from analytical grade raw materials of Na<sub>2</sub>CO<sub>3</sub>, K<sub>2</sub>CO<sub>3</sub>, MgO, CaCO<sub>3</sub>, H<sub>3</sub>BO<sub>3</sub>, CaHPO<sub>4</sub>·2(H<sub>2</sub>O) and Belgian quartz sand were melted in a platinum crucible for 3 h at 1360 °C, cast, annealed, crushed and remelted to ensure homogeneity. One half of the glass bars were cut into plates and the rest was crushed and sieved into powder with size less than 45 µm.

Differential thermal analysis (TGA/SDTA851<sup>e</sup> from Mettler Toledo) was used to measure the temperatures for glass transformation, onset of crystallization and liquidus. Parameters describing the crystal nucleation, shape and dimensionality were determined from the information from DTA. The samples were heated in alumina crucibles in flowing (50 cm<sup>3</sup>/min) dry nitrogen using 15 mg of glass powder (<45 µm) which was heated up to 1400 °C with heating rates of 15, 20, 30 and 40 °C/min.

The crystallization tendency at temperature ranges suggested by DTA were studied by heat-treating the glass plates in a tube furnace in nitrogen atmosphere. The plates were pushed into the preheated furnace at the specified temperature for 1 h, then rapidly removed and freely cooled to room temperature. The crystalline phases in the plates were studied with X-ray diffraction analysis (X'Pert by Philips) and scanning electron microscopy, SEM/EDX (LEO Vantage).

Low temperature viscosities of the glasses were measured with hot stage microscopy, HSM (Misura 3.0 by Expert). The sample was pressed into a cylinder with dimensions 3 mm × 3 mm from the powdered glass. Profile of the sample

heated with 5 °C/min to 1200 °C was imaged at every 5 °C. The obtained shrinkage curve calibrated with a standard glass of known viscosity (Standardglas I, HVG Germany) was used to measure the low temperature viscosities. High temperature viscosities were measured with a rotation viscometer at the Glass Research Institute Glafo, Sweden.

## 3. Results and discussion

The temperatures of glass transformation ( $T_g$ ), onset of crystallization ( $T_x$ ), crystallization peak ( $T_p$ ) and liquidus ( $T_l$ ) obtained from the DTA graphs as well as the calculated glass stability values,  $K_{gl}$  and  $T_{gr}$ , are given in Table 2.  $K_{gl}$  and  $T_{gr}$  were calculated using the equations:  $K_{gl} = (T_x - T_g)/(T_l - T_p)$  and  $T_{gr} = T_g/T_l$ .<sup>14,15</sup> According to the transformation and crystallization temperatures the experimental glasses can be divided into two groups: (1) glasses with transformation temperature around 500 °C and onset of crystallization below 750 °C, and (2) glasses with transformation temperature between 550 and 600 °C and onset of crystallization around 900 °C. The liquidus temperatures given by DTA indicate that at high temperatures all the experimental glasses crystallize between 1100 and 1200 °C. Glasses belonging to the second group have higher  $T_x$  and show high  $K_{gl}$  values, thus having higher stability against crystallization than the glasses with the lower  $T_x$  values. The glasses belonging to the second group are more stable against crystallization also according to the  $T_{gr}$  values. Glasses 45S5, 7-04 and 22-04 show  $T_{gr}$  values lower than 0.58. This would mean that these glasses show internal nucleation.<sup>14</sup> Although both stability parameters give similar trends, the  $K_{gl}$  proposed by Hruby is likely to describe the stability of bioactive glasses better as it takes into account crystallization temperature. The  $K_{gl}$  parameter has also been reported to correlate with the glass-forming tendency, as estimated by critical cooling rates.<sup>18</sup> Thus  $K_{gl}$  parameter can be used to compare different glass compositions suitable for fiber drawing directly from melt.

Activation energy, Avrami constant and the primary crystal type formed at crystallization temperature are given in Table 3. Fig. 1 shows the lines used for the determination of the activation energy for crystallization,  $\Delta E$ , according to the modified Kissinger equation.<sup>15</sup> The y-axis  $\ln(\beta/T_p - T_0)$  gives the ratio between the heating rate ( $\beta$ ) and observed peak temperatures from DTA and the x-axis  $1000/T_p$  is the inversed peak temperature. The activation energy was used to calculate the Avrami

Table 1  
Glass compositions (wt.%)

Glass	Na <sub>2</sub> O	K <sub>2</sub> O	MgO	CaO	B <sub>2</sub> O <sub>3</sub>	P <sub>2</sub> O <sub>5</sub>	SiO <sub>2</sub>
45S5 <sup>a</sup>	24.5	0	0	24.5	0	6	45
07-04	15	0	6	25	2	1	51
22-04	25	0	0	15	2	2	56
10-04	10	3.75	4.5	22.5	3	4	52.25
23-04	5	11.25	4.5	20	2	1	56.25
29-04	10	0	4.5	20	3	0	62.5
1-98 <sup>b</sup>	6	11	5	22	1	2	53

<sup>a</sup> Reference glass from Hench.<sup>1</sup>

<sup>b</sup> Reference glass from Ylänen et al.<sup>5</sup>

Table 2

Temperatures (°C) of glass transformation ( $T_g$ ), onset of crystallization ( $T_x$ ), crystallization peak ( $T_p$ ) and liquidus ( $T_l$ ) obtained from DTA (heating rate 15 °C/min) as well as the calculated glass stability values,  $K_{gl}$ <sup>13</sup> and  $T_{gr}$ <sup>14</sup>

Glass	$T_g$	$T_x$	$T_p$	$T_l$	$K_{gl}$	$T_{gr}$
45S5	532	655	708	1180	0.26	0.55
7-04	512	747	768	1130	0.65	0.56
22-04	469	676	728	1130	0.51	0.53
10-04	570	910	943	1160	1.57	0.59
23-04	590	916	953	1120	1.95	0.62
29-04	580	892	940	1160	1.42	0.60
1-98	590	910	954	1100	2.19	0.63

Table 3

Activation energy for crystal growth ( $\Delta E$ ) and Avrami constant ( $n$ ) measured by DTA and crystal types identified with XRD (NCS = sodium-calcium-silicate, CS = wollastonite)

Glass	$\Delta E$ [kJ mol <sup>-1</sup> ]	$n$	Crystal type
45S5	293	1.06	NCS
7-04	310	2.13	NCS
22-04	197	1.54	NCS
10-04	122	2.58	CS
23-04	311	2.41	CS
29-04	277	1.75	CS
1-98	281	1.38	CS

constant,  $n$ , describing the dimensionality of crystal growth according to equation<sup>15</sup>

$$n = \frac{2.5 RT_p^2}{\Delta \tau_{FWHM} \Delta E}$$

where  $\Delta \tau$  is the full width of the DTA exothermic peak at its half maximum,  $\Delta E$  is the activation energy and  $R$  is the gas constant. The calculated Avrami constants indicate that surface crystallization is dominant in all the experimental glasses. Bulk crystallization is reported to occur when the Avrami constant is higher than three.<sup>17</sup> Glasses 45S5, 7-04 and 22-04 show surface crystallization according to Avrami constant values but bulk crystallization according to  $T_{gr}$ .

X-ray analysis of the heat-treated samples gives sodium-calcium-silicate crystals (NCS) in the glasses crystallizing at the lower temperatures (Tables 2 and 3). Due to the similar patterns of the different sodium-calcium-silicates, the exact crystal type could not be identified with certainty. However, the best match was accomplished with the standard PDF 79.1087 representing  $\text{Na}_2\text{O} \cdot 2\text{CaO} \cdot 3\text{SiO}_2$  crystals. The SEM image in Fig. 2 of the cross-section of Glass 45S5 heat-treated at 900 °C for 1 h shows very small crystals in the glass surface, and a larger crystalline network pattern in the bulk. The boundaries and the interior of the network were found to have different chemical compositions according to the EDX analysis. The SEM image suggests that the glass has first undergone a liquid–liquid phase separation after which both the interface and the interior have crystallized. This crystallization process could be interpreted as internal nucleation, thus giving bulk crystallization. This is in

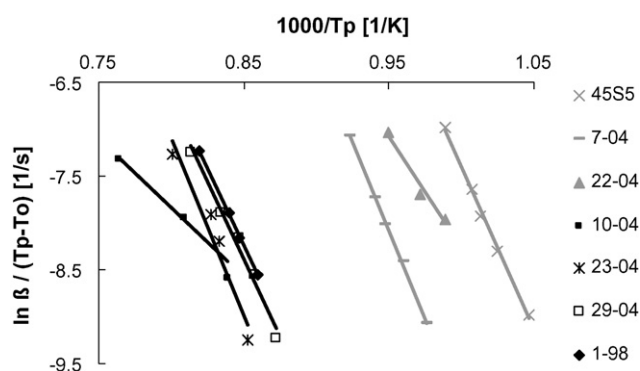


Fig. 1. Determination of  $\Delta E/R$  using the modified Kissinger method.<sup>15</sup>

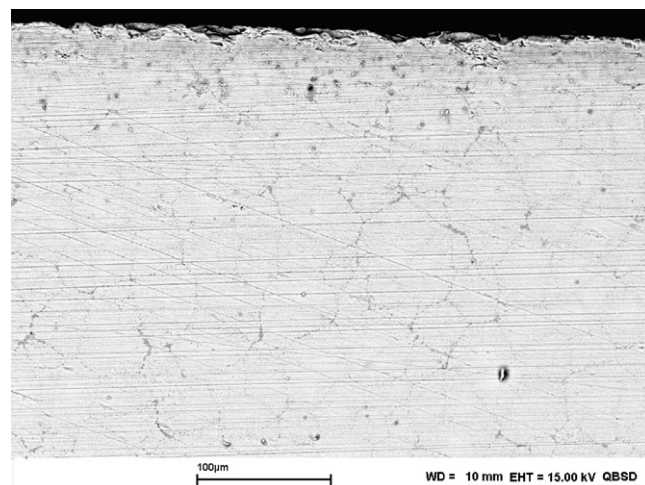


Fig. 2. SEM image of cross-section of heat-treated (1 h at 900 °C) Glass 45S5.

accordance with the  $T_{gr}$  value for the glass. The suggested surface crystallization by the Avrami constant is assumed to depend on the small particle size used to measure the different peak characteristics. In systems with bulk crystallization small particles can give surface crystallization.<sup>19</sup>

Crystals formed in Glasses 10-04, 23-04, 29-04 and 1-98 were identified as wollastonite ( $\text{CaCO}_3$ ) according to XRD analysis. A cross-section of the heat-treated (1 h at 900 °C) plate of Glass 1-98 is given in Fig. 3. Big needles of wollastonite have grown from the surface into the glass, thus verifying the surface crystallization suggested by the Avrami constant and the  $T_{gr}$  value.

Viscosity–temperature curves for the glasses are given in Fig. 4. The sintering and fiber drawing ranges outlined coincide with the crystallization and liquidus temperatures for the glasses showing NCS formation. However, for the glasses showing wollastonite formation, crystallization commences at temperatures high enough to allow viscous flow sintering. The figure also indicates that a fiber drawing from melt could be accomplished for wollastonite type glasses.

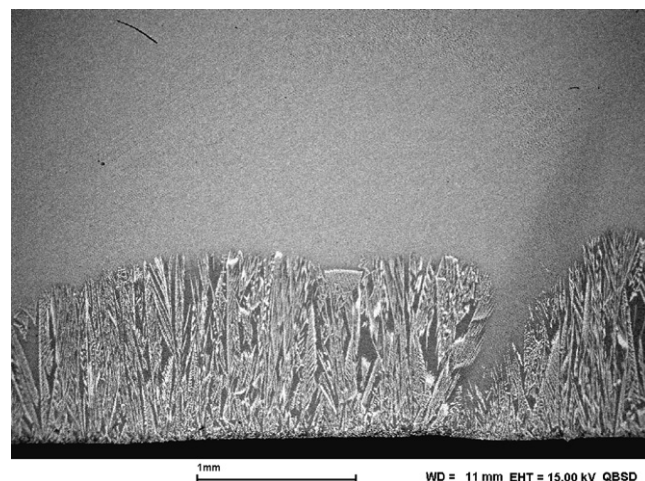


Fig. 3. SEM image of cross-section of heat-treated (1 h at 900 °C) Glass 1-98.

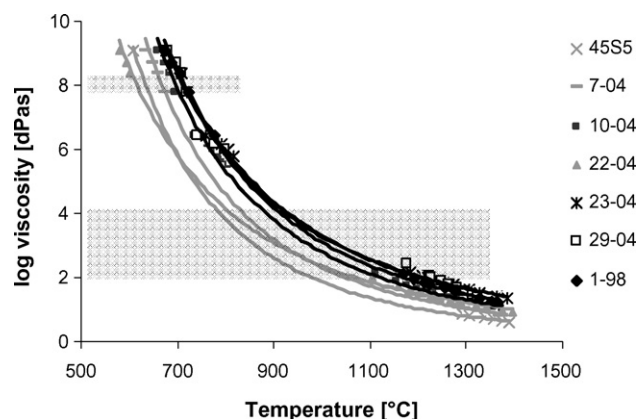


Fig. 4. Viscosity curves obtained by HSM and rotation viscometer. The viscosities corresponding sintering (upper) and fiber drawing (lower) are marked with grey areas.

#### 4. Conclusions

All the experimental glasses were found to phase separate during heat-treatments, but clearly within two distinct temperature ranges typical for the primary crystalline phase formed in crystallization, i.e. sodium-calcium-silicate or wollastonite. The sodium-calcium-silicate forming glasses had onset of crystallization below 750 °C while wollastonite type glasses crystallized around 900 °C. The glass stability values indicated that wollastonite type glasses should be more stable against crystallization. Crystallization characteristics, expressed as the reduced glass transformation value and the Avrami constant, suggest that surface crystallization is the main mode of phase separation in wollastonite type glasses. In sodium-calcium-silicate type glasses glass-to-glass phase separation and internal nucleation were observed. Viscosity values associated with viscous flow sintering or fiber drawing coincided with crystallization for the sodium-calcium-silicate type glasses. Thus, when tailoring compositions for demanding glass-forming processes, such as sintering or fiber drawing, preferably compositions showing wollastonite type crystallization should be considered.

#### Acknowledgements

The National Centre of Excellence Programme by the Academy of Finland, Combio Technology Programme by the Finnish National Technology Agency and Biomaterial Graduate School are acknowledged for financial support. Tampere University of Technology, University of Turku, University of Oulu,

Linvatec Biomaterials Ltd., Vivoxid Ltd., and Bioretec Ltd are acknowledged for collaboration.

#### References

- Hench, L. L., Bioceramics: from concept to clinic. *J. Am. Ceram. Soc.*, 1991, **74**(7), 1487–1510.
- El-Ghannam, A., Hamazawy, E. and Yehia, A., Effect of thermal treatment on bioactive glass microstructure, corrosion behavior,  $\zeta$  potential, and protein adsorption. *J. Biomed. Mater. Res.*, 2001, **55**, 387–395.
- Peitl, O., Zanotto, E. D. and Hench, L. L., Highly bioactive P2O<sub>5</sub>-Na<sub>2</sub>O-CaO-SiO<sub>2</sub> glass-ceramics. *J. Non-Cryst. Solids*, 2001, **292**, 115–126.
- Brink, M., The influence of alkali and alkaline earths on the working range for bioactive glasses. *J. Biomed. Mater. Res.*, 1997, **36**, 109–117.
- Ylänen, H. O., Helminen, T., Helminen, A., Rantakokko, J., Karlsson, K. H. and Aro, H. T., Porous bioactive glass matrix in reconstruction of articular osteochondral defect. *Ann. Chirurgiae. et Gynaecologiae*, 1999, **88**, 237–245.
- Itälä, A., Koort, J., Ylänen, H. O., Hupa, M. and Aro, H., Biologic significance of surface microroughening in bone incorporation of porous bioactive glass implants. *J. Biomed. Mater. Res. A*, 2003, **67**(2), 496–503.
- Arstila, H., Zhang, D., Vedel, E., Hupa, L., Ylänen, H. and Hupa, M., Bioactive glass compositions suitable for repeated heat-treatments. *Key Eng. Mat.*, 2005, **284–286**, 925–928.
- Fröberg, L., Hupa, L. and Hupa, M., Porous bioactive glasses with controlled mechanical strength. *Key Eng. Mat.*, 2004, **254–256**, 973–976.
- Cable, M., In *Classical Glass Technology in Materials Science and Technology—A Comprehensive Treatment*, ed. J. Zarzycki. VCH Verlagsgesellschaft, Weinheim, 1991.
- Arstila, H., Fröberg, L., Hupa, L., Vedel, E., Ylänen, H. and Hupa, M., The sintering range of porous bioactive glasses. *Glass Technol.*, 2005, **46**(2), 138–141.
- Shelby, J. E., *Introduction to Glass Science and Technology*. The Royal Society of Chemistry, Thomas Gramham House, 1997.
- Wallenberger, F. T. and Weston, N. E. Glass fibers from high and low viscosity melts. *Mat. Res. Soc. Symp. Proc.*, Vol 702, Materials Research Society, 2002.
- Hruby, A., Evaluation of glass-forming tendency by means of DTA [differential thermal analysis]. *J. Phys.*, 1972, **B22**, 1187–1193.
- Zanotto, E. D., Isothermal and adiabatic nucleation in glass. *J. Non-Cryst. Solids*, 1987, **89**, 361–370.
- Augis, J. A. and Bennett, J. E., Calculation of the avrami parameters for heterogeneous solid state reactions using modification of the Kissinger method. *J. Thermal Anal.*, 1978, **13**, 283–292.
- Marotta, A., Buri, A. and Valenti, G. L., Crystallization kinetics of gehlenite glass. *J. Mater. Sci.*, 1978, **13**, 2483.
- Marotta, A., Saiello, F., Branda, F. and Buri, A. J., Activation energy for the crystallization of glass from DDTA curves. *Mater. Sci.*, 1982, **17**, 105.
- Cabral, A. A., Fredericci, C. and Zanotto, E. D., A test of the Hruby parameter to estimate glass-forming ability. *J. Non-Cryst. Solids*, 1997, **219**, 182–186.
- Xu, X. J., Ray, C. S. and Day, D. E., Nucleation and crystallization of Na<sub>2</sub>O-2CaO-3SiO<sub>2</sub> glass by differential thermal analysis. *J. Am. Ceram. Soc.*, 1991, **74**(5), 909–914.